scientific reports

Check for updates

OPEN

SARS-CoV-2 infection causes a decline in renal megalin expression and affects vitamin D metabolism in the kidney of K18-hACE2 mice

Yoshifumi Kurosaki[1,2], Toshihide Matsumoto[2,3], Takayuki Uematsu[4], Fumitaka Kawakami[2,5], Rei Kawashima[2,6], Shun Tamaki[2,6], Motoki Imai[2,7], Takafumi Ichikawa[2,6], Naohito Ishii[1,2], Hidero Kitasato[2,8], Hideaki Hanaki[9] & Makoto Kubo[2,8]✉

Patients with coronavirus disease 2019 (COVID-19) often experience acute kidney injury, linked to disease severity or mortality, along with renal tubular dysfunction and megalin loss in proximal tubules. Megalin plays a crucial role in kidney vitamin D metabolism. However, the impact of megalin loss on vitamin D metabolism during COVID-19 is unclear. This study investigated whether severe acute respiratory syndrome coronavirus 2 (SARS-CoV-2) infection reduces megalin expression in proximal tubules and its subsequent effect on vitamin D metabolism in mice expressing human angiotensin converting enzyme 2 (K18-hACE2 mice). Histological and immunohistochemical staining analyses revealed glomerular and capillary congestion, and elevated renal neutrophil gelatinase-associated lipocalin levels, indicative of acute kidney injury in K18-hACE2 mice. In SARS-CoV-2-infected mice, immunohistochemical staining revealed suppressed megalin protein levels. Decreased vitamin D receptor (VDR) localization in the nucleus and increased mRNA expression of VDR, CYP27B1, and CYP24A1 were observed by quantitative PCR in SARS-CoV-2-infected mice. Serum vitamin D levels remained similar in infected and vehicle-treated mice, but an increase in tumor necrosis factor-alpha and a decrease in IL-4 mRNA expression were observed in the kidneys of the SARS-CoV-2 group. These findings suggest that megalin loss in SARS-CoV-2 infection may impact the local role of vitamin D in kidney immunomodulation, even when blood vitamin D levels remain unchanged.

Coronavirus disease 2019 (COVID-19), caused by severe acute respiratory syndrome coronavirus 2 (SARS-CoV-2), has become a global pandemic. Studies have reported a correlation between acute kidney injury (AKI) and overall disease severity or mortality[1,2]. A systematic review and meta-analysis of 20 cohorts with COVID-19-associated AKI (CoV-AKI) reported a prevalence of AKI ranging from 0.5 to 80% (with an average of 17%) and 77% of the patients with AKI exhibited severe COVID-19 manifestation[3]. Some mechanisms for kidney injury in COVID-19 have been proposed, including direct infection, inflammatory injury followed by a cytokine storm, and ischemic injury caused by multiorgan failure[4,5]; however, the cause of kidney injury in COVID-19 remains unclear. Previous studies have reported that acute tubular injury is the main finding in patients with CoV-AKI[6–8]. A postmortem study patients revealed significant acute tubular injury in all patients[9]. Low-grade proteinuria has been detected in patients with COVID-19 without AKI[10,11]. Proteinuria during hospitalization was significantly associated with an increased risk of death[12], which suggests that renal tubular dysfunction

[1]Department of Medical Laboratory Sciences, School of Allied Health Sciences, Kitasato University, 1-15-1 Kitasato, Sagamihara 252-0373, Japan. [2]Regenerative Medicine and Cell Design Research Facility, School of Allied Health Sciences, Kitasato University, 1-15-1 Kitasato, Sagamihara 252-0373, Japan. [3]Department of Pathology, School of Allied Health Sciences, Kitasato University, 1-15-1 Kitasato, Sagamihara 252-0373, Japan. [4]Biomedical Laboratory, Division of Biomedical Research, Kitasato University Medical Center, 6-100 Arai, Kitamoto 364-8501, Japan. [5]Department of Health Administration, School of Allied Health Sciences, Kitasato University, 1-15-1 Kitasato, Sagamihara 252-0373, Japan. [6]Department of Biochemistry, School of Allied Health Sciences, Kitasato University, 1-15-1 Kitasato, Sagamihara 252-0373, Japan. [7]Department of Molecular Diagnostics, School of Allied Health Sciences, Kitasato University, 1-15-1 Kitasato, Sagamihara 252-0373, Japan. [8]Department of Environmental Microbiology, Kitasato University Graduate School of Medical Sciences, 1-15-1 Kitasato, Sagamihara 252-0373, Japan. [9]Infection Control Research Center, Ōmura Satoshi Memorial Institute, Kitasato University, 5-9-1 Shirokane, Minato-ku, Tokyo 108-8641, Japan. ✉email: kuboma@kitasato-u.ac.jp

could be related to an increase in disease severity in patients with COVID-19, irrespective of the presence of AKI.

There are correlations between serum vitamin D levels and COVID-19 severity[13]. Studies have reported a protective role of vitamin D against respiratory infection[14], including COVID-19[15]. Vitamin D has been suggested as an immunomodulator that affects the innate and adaptive immune systems[16]. However, studies evaluating the efficacy of vitamin D supplementation in patients with moderate-to-severe COVID-19 have reported inconsistent results[17]. In the liver, vitamin D transported from the diet and skin via circulation is metabolized to 25-hydroxyvitamin D (25(OH)D). The 25(OH)D is filtered by the renal glomerulus and reabsorbed by proximal tubules wherein 25(OH)D is hydroxylated by 1α-hydroxylase, the enzyme of cytochrome P450 family 27 subfamily B member 1 (CYP27B1), to its active form, 1,25-dihydroxyvitamin D ($1,25(OH)_2D$)[18]. Activated $1,25(OH)_2D$ binds to the vitamin D receptor (VDR), leading to the expression of VDR target genes that regulate calcium concentration[19], and mediates the effects of immunomodulation, anti-inflammation[20], and anti-proliferation[21]. In contrast, $1,25(OH)_2D$ is hydroxylated by 24-hydroxylase, an enzyme of the cytochrome P450 family 24 subfamily A member 1 (CYP24A1), to form $1,24,25\ (OH)_3D$, which is less active than $1,25(OH)_2D$ at activating VDR[22]. Thus, the kidneys play a critical role in maintaining active blood vitamin D levels. The development of AKI[23] and chronic kidney disease (CKD)[24] has been associated with vitamin D disorders. Because vitamin D is fat-soluble, most circulating 25(OH)D binds to vitamin D-binding proteins in the blood. This protein-bound 25(OH)D complex is internalized into the proximal tubules by the renal endocytic receptors megalin and cubilin[25]. Therefore, receptor-mediated endocytosis is essential for maintaining vitamin D homeostasis.

Megalin is located on the apical membrane of the proximal tubule epithelial cells and plays a critical role in the reabsorption of low molecular weight proteins[26,27]. Megalin internalizes carrier protein-bound vitamins, including vitamin D-binding protein, which is essential for vitamin D homeostasis in vivo; hence, megalin knockout mice show low plasma 25(OH)D levels and urinary loss of the vitamin[28]. Recent studies have reported decreased megalin expression in kidney biopsies from patients with COVID-19[29] and in monolayers of primary human kidney cells[30]. Therefore, decreased megalin expression and abnormal vitamin D metabolism may be associated with the severity of COVID-19. However, the relationship between renal megalin expression and vitamin D metabolism in patients with COVID-19 remains unclear.

In this study, we examined whether COVID-19 infection decreases megalin expression in the proximal tubule and its subsequent effect on vitamin D metabolism in a COVID-19 infection model mice, transgenic mice were driven by human angiotensin-converting enzyme 2 (ACE2) into mouse epithelial cells under the control of the human cytokeratin 18 (K18) promoter (K18-hACE2 mice).

Results

SARS-CoV-2-infected mice showed interruption of renal circulation in histological analysis

In the present study, the kidneys of some SARS-CoV-2 infected mice were pale, suggesting renal congestion (Fig. 1A). Histological analysis revealed glomerular (Fig. 1B,C,E) and capillary (Fig. 1B,C,F) congestion in the kidneys of SARS-CoV-2-infected mice. In addition, Masson's Trichrome staining showed that renal tissue in infected mice exhibited moderate tubulointerstitial fibrosis compared with vehicle-treated mice and that red blood cells were observed in the interstitial region of the renal cortex of the SARS-CoV-2-infected mice, suggesting bleeding (Fig. 1D,G). An increase in the AKI marker neutrophil gelatinase-associated lipocalin (NGAL) was observed on day two after SARS-CoV-2 infection and was maintained until day seven but decreased compared with day two (Fig. 2A). Kidney injury molecule-1 (Kim-1), another AKI maker, also exhibited increased levels on day two after infection (Fig. 2B), but this increase in the kidneys of infected mice was mild compared to that in rhabdomyolysis-induced AKI mice (Supplemental Fig. 1). Since some research has reported that cell cycle arrest and DNA injury in proximal tubule cells are observed in the AKI model animals[31–33], we examined the proliferating cell nuclear antigen (PCNA) and γ phosphorylated form of the histone H2AX (γH2AX) expression, which are proliferation and DNA injury markers, respectively, in *Lotus Tetragonolobus* lectin (LTL)-positive tubule. The number of PCNA-positive cells was decreased (Fig. 2C), whereas that of γH2AX-positive cells was elevated in the LTL-positive tubules of infected mice on day seven (Fig. 2D). These results suggest that SARS-CoV-2 infection causes AKI mainly by interrupting the renal circulation.

In situ hybridization analysis revealed that SARS-CoV-2 RNA was detected in the lungs but not in the kidneys of the infected mice (Fig. 3A). In contrast, the viral spike protein was detected in the renal cortex (Fig. 3B).

Megalin expression in renal cortex of SARS-CoV-2-infected mice

Periodic acid-Schiff staining showed that the tubule brush border had less contrast in the infected mice (Fig. 4A,B). We then evaluated megalin expression in the kidneys of the infected mice. Megalin protein levels declined significantly in the infected kidney on day seven but not on day two (Fig. 4C,D). Moreover, the mRNA levels of *Lrp2*, which encodes megalin, were elevated in the renal cortex of the SARS-CoV-2-infected mice on day seven (Fig. 4E).

Effect of SARS-CoV-2 infection on Vitamin D metabolism

Because megalin is a key player in vitamin D metabolism in the kidney, we evaluated whether megalin decline affected vitamin D metabolism in the kidney. In the analysis of vitamin D activation factors, most VDR-positive nuclei were observed in the distal tubule and much fewer were seen in the proximal tubule in vehicle-treated mice (Supplemental Fig. 2). In SARS-CoV-2-infected mice, VDR localization to the nucleus was significantly decreased (Fig. 5A,B), whereas the mRNA levels of *VDR* was upregulated (Fig. 5C). The protein levels of CYP27B1 and CYP24A1 in the SARS-CoV-2-infected mice were similar to those in the vehicle-treated mice (Fig. 5D,F). In contrast, the mRNA levels of *CYP27B1* and *CYP24A1* in the renal cortex were upregulated in infected mice (Fig. 5E,G). We then decided to determine blood 25(OH)D and $1,25(OH)_2D$ levels to evaluate

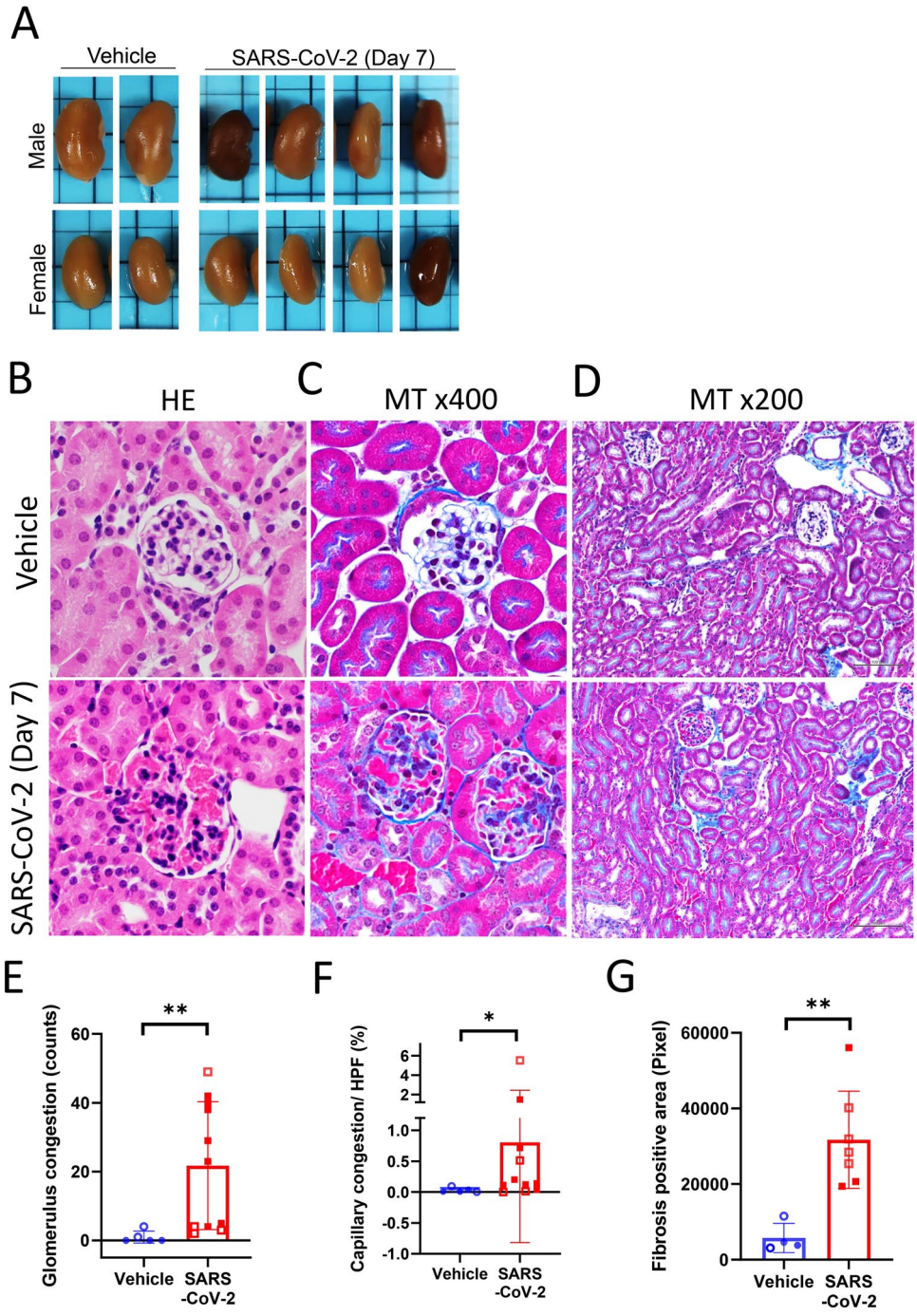

Fig. 1. SARS-CoV-2 infection causes renal congestion and interruption of circulation. (**A**) Appearances of SARS-CoV-2-infected kidneys. Hematoxylin (**B**) and Masson's trichrome staining (**C** and **D**) were performed to evaluate the morphological changes in the kidney of SARS-CoV2-infected mice seven days after infection. (**E**–**F**) Congestion in glomeruli (**E**) or capillaries (**F**) and the fibrosis positive in Masson's trichrome staining (**G**) were semi-quantified as described in Methods. Each data points from male and female mice were shown with closed and opened symbols.

whether SARS-CoV-2 infection affects vitamin D metabolism in the whole body. Serum vitamin D levels in infected mice did not change compared with those in vehicle mice (Fig. 6A,B). Then, we examined mRNA expression of tumor necrosis factor α (TNF-α) to evaluate the effect of the abnormality of vitamin D metabolism on the local inflammation and found TNF-α expression was elevated in the kidney of infected mice (Fig. 6C). Additionally, a decrease in IL-4 expression and an increase in IL-10 mRNA expression were observed in the kidneys of the SARS-CoV-2 group (Fig. 6D,E).

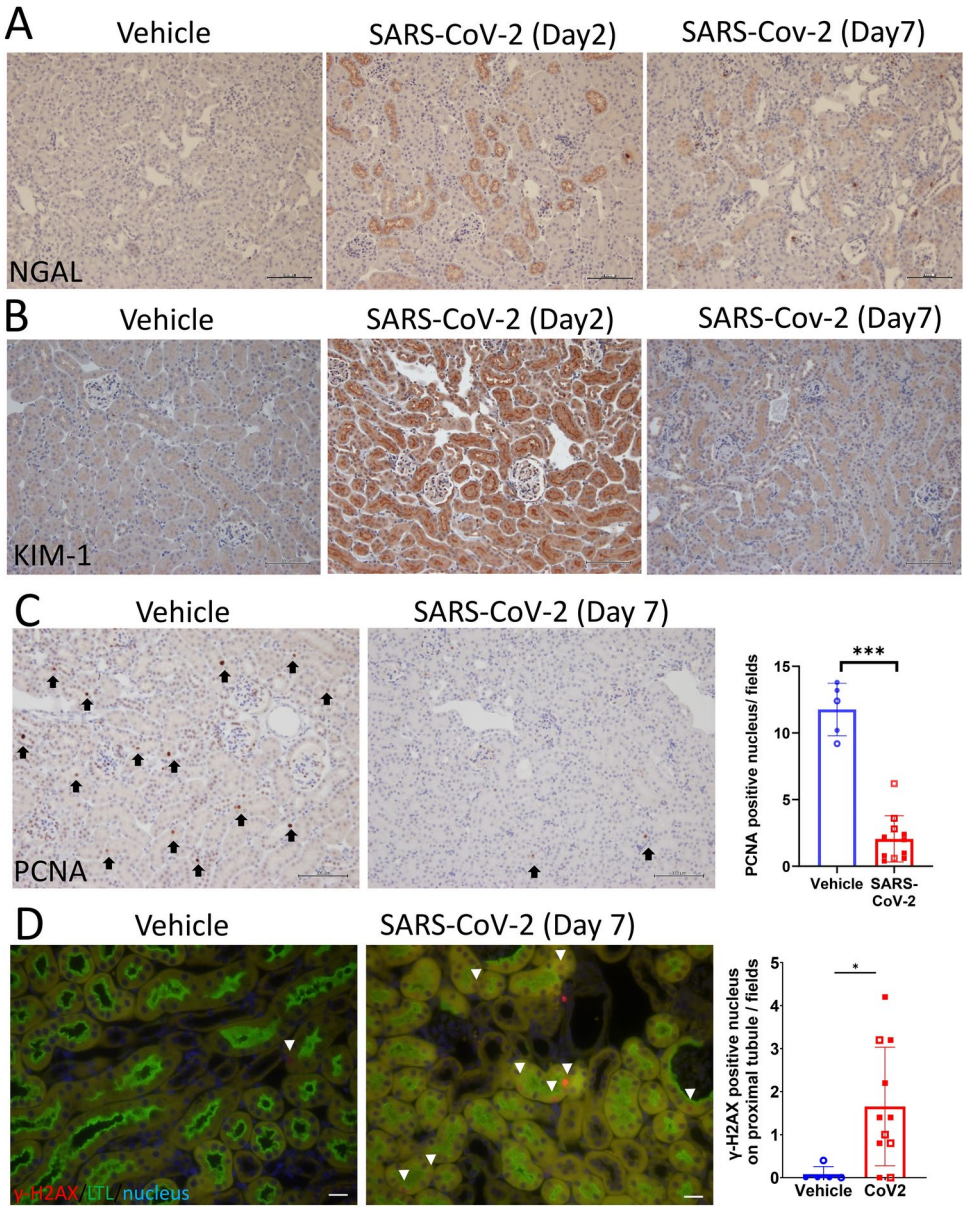

Fig. 2. SARS-CoV-2 infection causes AKI and cell cycle arrest in proximal tubules of hACE2-Tg mice. NGAL (**A**) and Kim-1 (**B**) immunohistochemistry two or seven days after SARS-CoV-2 or vehicle treatment of the renal cortex. Representative PCNA (**C**) and γH2AX (**D**) (red) on LTL (green)-positive tubule-stained images seven days after treatment and quantification of positive cells per field. The arrows in **C** indicate the positive PCNA nuclei, and the white arrowheads in **D** indicate the positive nuclei in the LTL-positive tubules (proximal tubules). Each data points from male and female mice were shown with closed and opened symbols. Values are the means ± SD (n = 5–11/group).

Sex difference in AKI of SARS-CoV-2 infected mice

To see the sex difference in this study, we summarized the parameters which showed the change in SARS-CoV-2-infected mice. In infected mice, all parameters, except luminance of brush border, showed no tendency between male and female (Table 1).

Discussion

AKI in patients with COVID-19 has been reported to be associated with in-hospital mortality[2,11], intensive care unit admission rate[10], and mechanical ventilation rate[34], whereas the mechanisms underlying CoV-AKI have not been clarified. In hACE2-Tg mice, SARS-CoV-2 infection caused glomerular and capillary congestion and bleeding in the interstitial region. SARS-CoV-2 infection induces vasoconstriction and a state of hypercoagulability, which lead to the formation of microthrombi and renal microvasculature injury, causing acute kidney injury[9,35]. Additionally, NGAL and Kim-1 expression was elevated on day two in infected

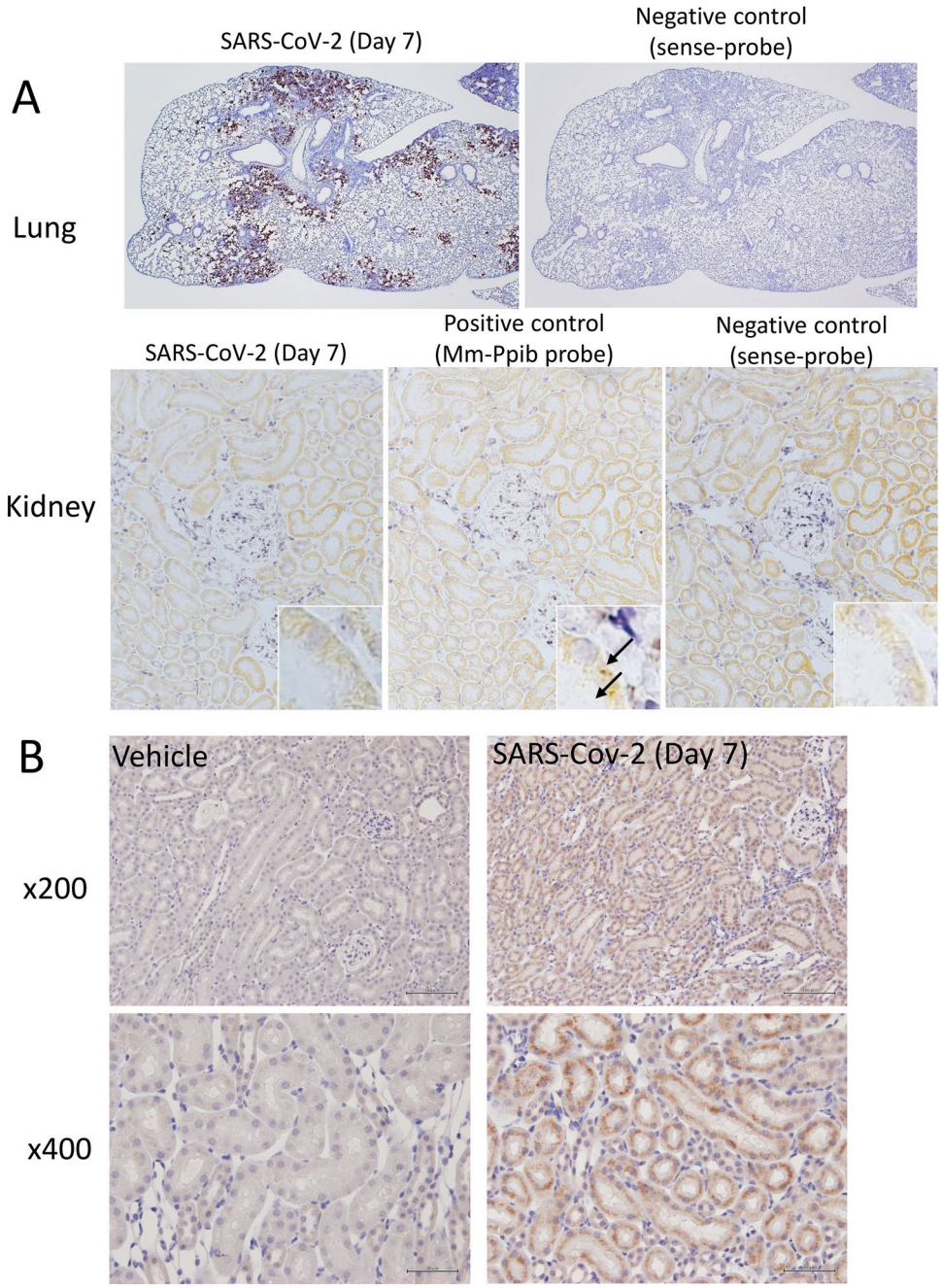

Fig. 3. SARS-CoV-2 spike protein is detected, but not viral RNA, in the infected kidney. (**A**) In situ hybridization images of the lung (×40 magnification) or renal cortex (×200 magnification) in SARS-CoV-2-infected mice on day seven. A sense probe was used for the negative control, and the Mm-Ppib probe was used for the positive control (an arrow indicates positive staining with the Mm-Ppib probe). (**B**) Representative immunochemistry images of spike protein taken with ×200 or ×400 magnification.

mice. DNA injury and cell cycle arrest were also observed in SARS-CoV-2-infected mice. These results show that SARS-CoV-2 infection causes AKI in hACE2-Tg mice by impairing the microcirculation. Furthermore, we evaluated the possibility of a direct viral infection. However, no SARS-CoV-2 mRNA was detected in the infected kidneys, suggesting that the main cause of AKI is not direct viral infection in the kidneys of infected mice. One of the limitations of the present study is that, because we used only one dose of the virus, we cannot exclude the possibility of higher-dose viral infection in the kidney. Researchers have reported that viral RNA can be detected in the kidneys and urine of patients with severe COVID-19[29,36].

Periodic acid-Schiff staining revealed mild injury to the tubular brush border. We evaluated the megalin expression in SARS-CoV-2-infected mice. On day two after infection, megalin expression was not altered compared to that in vehicle mice but decreased significantly on day seven. In infected mice, the viral spike

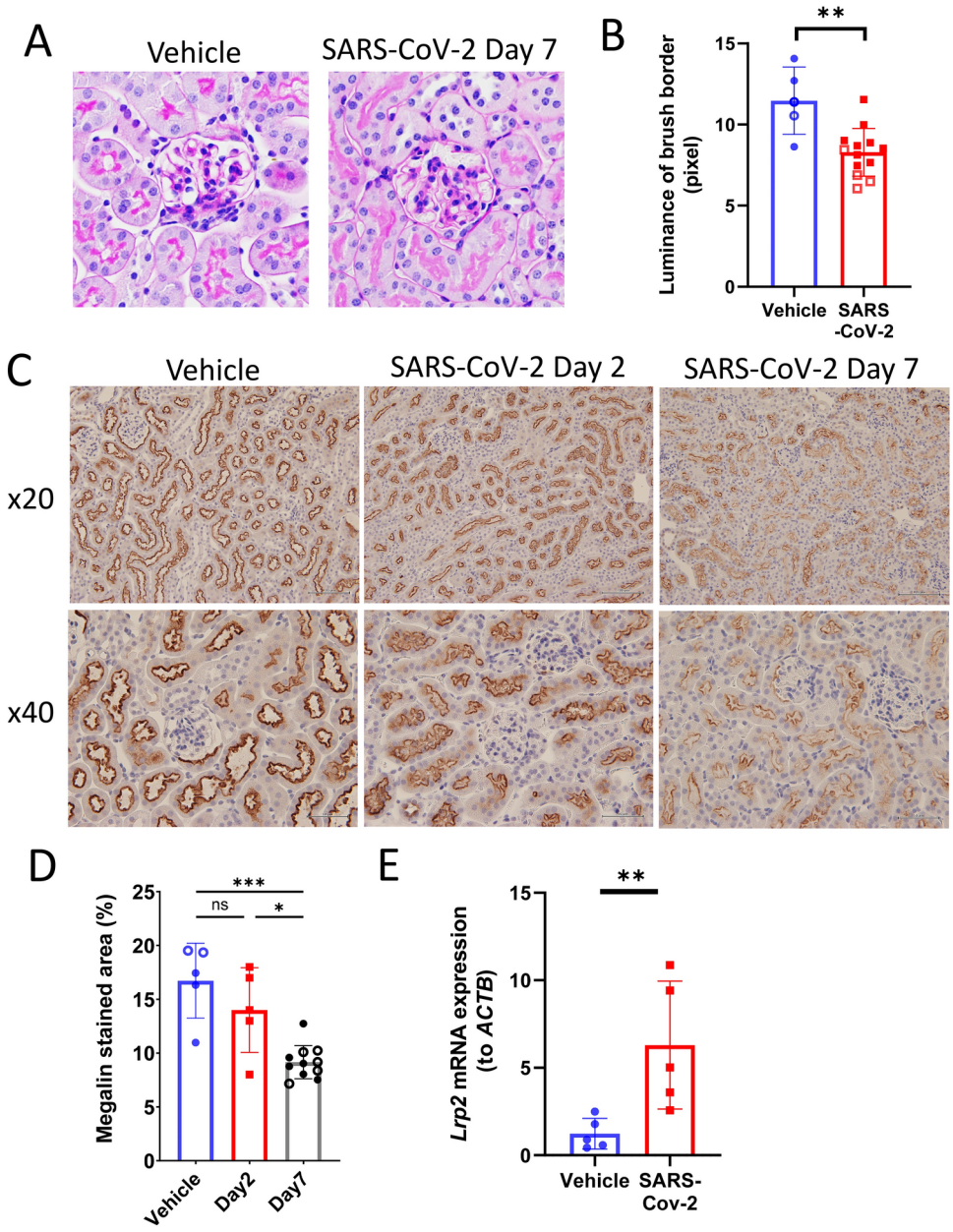

Fig. 4. SARS-CoV-2 infection suppresses megalin expression in the proximal tubules. (**A**) Periodic acid-Schiff staining was performed on the kidney of SARS-CoV-2-infected mice on day seven, and (**B**) the luminance of the brush border in the cortex was quantified as described in Methods. (**C**) Representative images showing renal megalin expression two or seven days after SARS-CoV-2 infection. (**D**) The graph depicts a quantitative representation of the megalin staining area in C. Values are mean ± SD (n = 5–11/group). Each data point from male and female mice were shown with closed and opened symbols. (**E**) Lrp2 (encoding megalin) mRNA in the kidney seven days after infection was quantified (means ± SD, n = 5/group).

protein was detected in the tubules, although viral RNA was not detected in the kidneys using in situ hybridization. ACE2 is a receptor for the SARS-CoV-2 spike protein, permitting the internalization of the virus into target cells[37] and is highly expressed in renal tubular epithelial cells[38]. SARS-CoV-2 shows limited binding to ACE2 in mice, which limits its use of as an animal model for COVID-19[37]. Therefore, it was suggested that the uptake of viral spike proteins observed in hACE2-Tg mice occurred through human ACE2 on the apical side of the proximal tubular cells (Supplemental Fig. 3). Thus, circulating spike protein may be internalized into the proximal tubule via ACE2. Spike protein has been detected in the urine of patients with COVID-19, indicating that the spike protein is filtered by the glomeruli[39]. In addition, spike proteins have been reported to be absorbed via megalin, which induces a decrease in megalin expression in the porcine proximal tubular cell line, LLCPK1[40]. Further evaluation using in vivo models is needed to prove that spike protein modulates megalin expression and proximal tubular cell functions. In contrast, megalin mRNA expression was elevated in

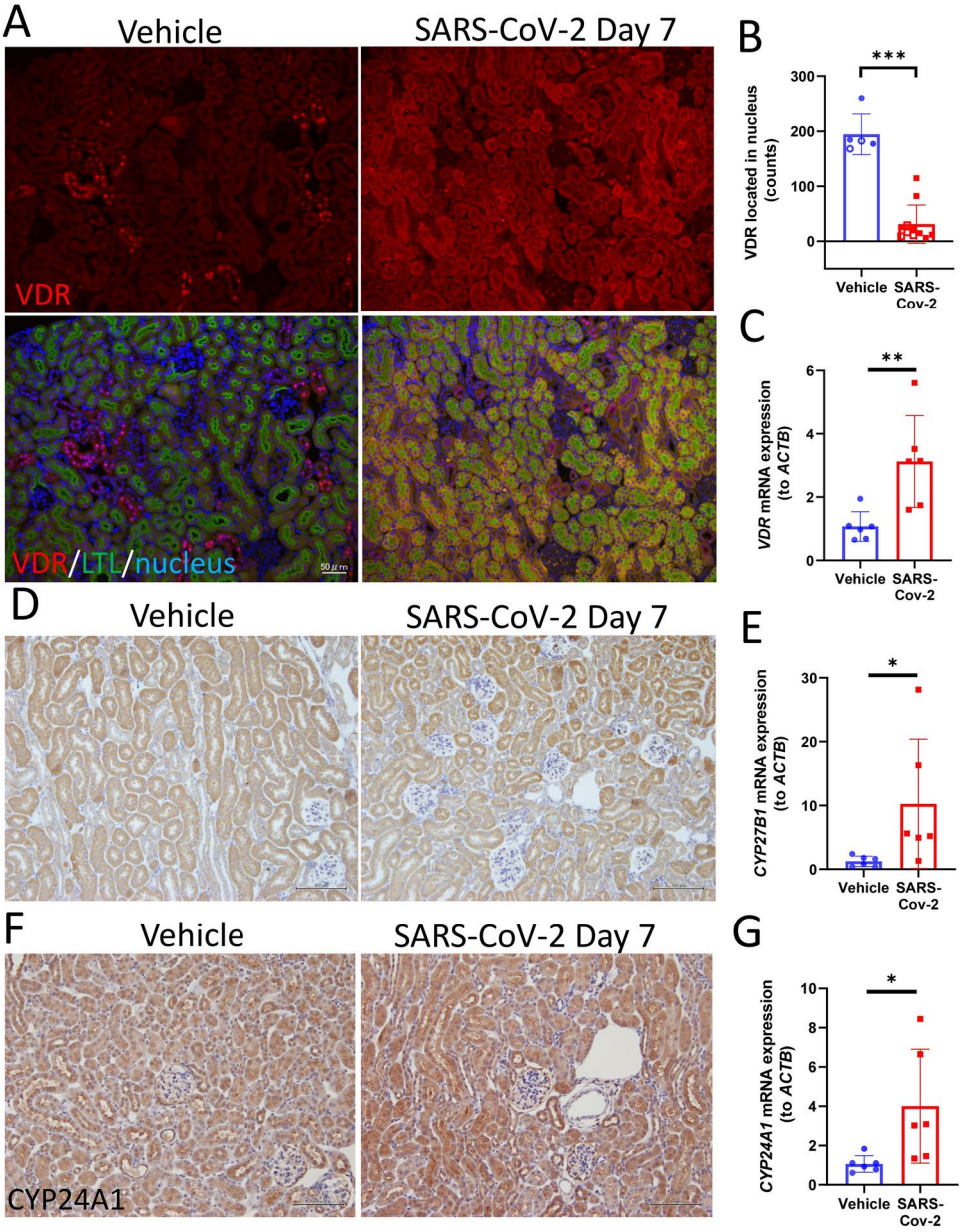

Fig. 5. SARS-CoV-2 infection induces abnormal vitamin D metabolism. (**A**) Representative immunofluorescence images of VDR (red: VDR, green: LTL, and blue: nuclei) in mouse kidneys seven days after SARS-CoV-2 or vehicle treatment and (**B**) quantification of positive nuclei per field. Each data from male and female mice were shown with closed and opened symbols. (**C**) *VDR* mRNA levels seven days after infection were quantified using qPCR (means ± SD, n = 6/group). (**D**, **F**) Representative immunohistochemistry images of CYP27B1 (**D**), and CYP24A1 (**F**) in mouse kidneys seven days after SARS-CoV-2. mRNA levels of *CYP27B1* (**E**) and *CYP24A1* (**G**) seven days after infection were quantified using qPCR (means ± SD, n = 6/group).

SARS-CoV-2-infected mice. Binding of ligands to megalin activates the intramembrane proteolysis of megalin, which negatively regulates megalin expression[41,42]. Therefore, it was suggested that a decrease in megalin protein levels induced megalin mRNA expression through intramembrane proteolysis of megalin as a negative feedback system. Indeed, megalin mRNA levels have been reported to increase when proteinuria induces a decline in megalin protein levels via shedding[43]. In the current study, urine was not collected due to biosafety regulations. Further studies to determine urinary megalin excretion in this model would help understand the mechanism of megalin decrease in the kidneys of SARS-CoV-2-infected mice.

Since reduced megalin protein levels were observed on day seven after infection, we evaluated the abnormality of vitamin D metabolism in mouse renal tubules. Although urinary vitamin D-binding proteins have been observed in megalin knockout mice[25], it was not possible to collect urine as stated above. VDR translocation and the expression of vitamin D metabolic enzymes in the kidneys were examined to evaluate whether reduced

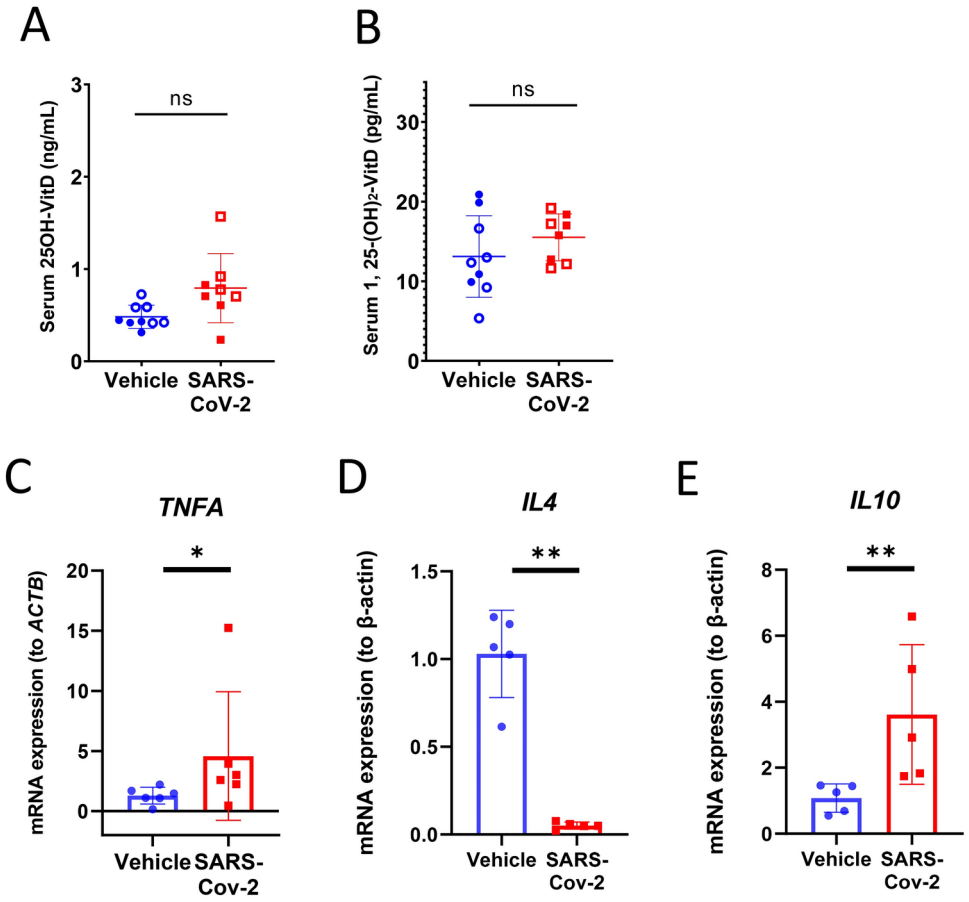

Fig. 6. SARS-CoV-2 infection shows no effect on serum vitamin D levels but affects local inflammation in the kidney. (**A**–**B**) Serum levels of 25OH-VitD (**A**) and 1,25-(OH)2-VitD (**B**) seven days after infection were determined using enzyme-linked immunosorbent assay (means ± SD, n = 8–9/group). Each data from male and female mice were shown with closed and opened symbols. (**C**) *TNFA* (encoding TNF-α), (**D**) *IL4*, and (**E**) *IL10* mRNA levels seven days after infection were quantified using qPCR (means ± SD, n = 5–6/group).

Parameters	*p*
Glomerulus congestion	0.2515
Capillary congestion	0.7879
Fibrosis area	0.6286
PCNA positive cells (proliferation)	0.1182
γ-H2AX positive cells (DNA injury)	0.4667
Luminance of brush border	< 0.05 (male > female)
Megalin expression	0.5273
VDR location in nucleus	0.4121

Table 1. Summarized sex difference in AKI of SARS-CoV-2-infected mice.

megalin levels affect the vitamin D metabolism in SARS-CoV-2-infected mice. Most VDR-positive nuclei were observed in the distal tubules of vehicle-treated mice, but a small part of them in the proximal tubules. This seemed to indicate that vitamin D activation in the proximal tubule might function in the distal tubule in a paracrine-like manner. A previous study has suggested that $1,25(OH)_2D$ activated in proximal tubule enters distal tubular cells by diffusion over their plasma membranes[44]. On the other hand, VDR translocation to the nucleus is suppressed in SARS-CoV-2-infected mice (Fig. 7). VDR translocated to the nucleus plays a critical role as a transcription factor and activates the transcription of genes associated with calcium homeostasis, vitamin D metabolism, including CYP24A1[19], and local immune modulators[45]. Therefore, decreased VDR translocation may affect the local immune system in the kidneys. In contrast, VDR mRNA levels were upregulated in the kidneys of the infected mice. A previous study reported elevated *VDR* mRNA in IRI-AKI mice[46], which is consistent with the results of this study. Although the expression levels of CYP24A1 and CYP27B1 proteins did not change in

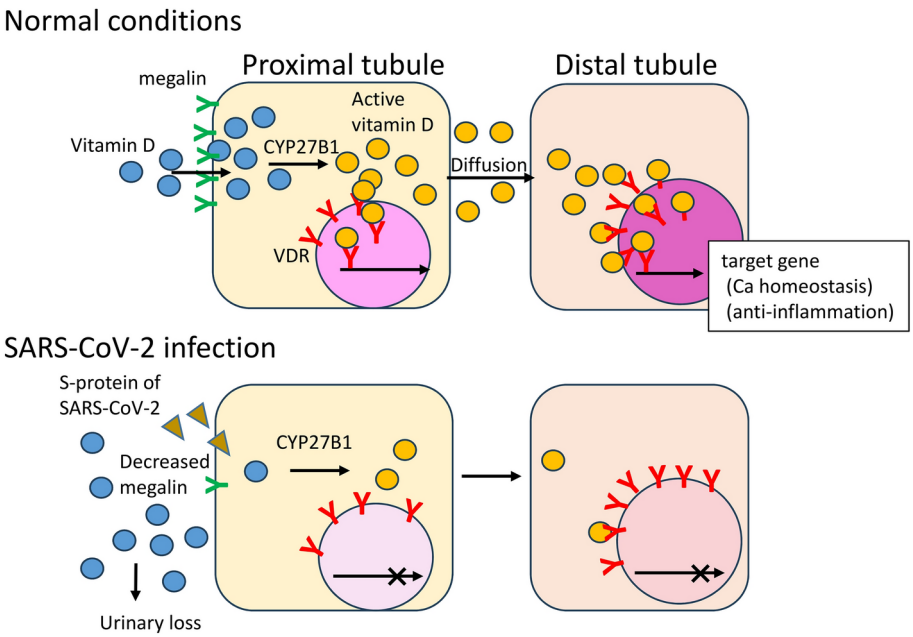

Fig. 7. A schematic hypothetical model for the impact of SARS-CoV-2 infection on vitamin D metabolism in renal tubules. Under the physiological conditions, vitamin D bound to DBP is filtered into the primary urine from which it is normally uptaken by megalin into proximal tubular cells. CYP27B1 catalyzed the conversion of the vitamin D into the active metabolite, $1,25(OH)_2D$, in proximal tubular cells. The activated vitamin D bound to VDR which translocate to nuclear and activates the transcription of vitamin D dependent genes in proximal tubular cells. Additionally, activated vitamin D enters distal tubular cells in paracrine manner and binds to VDR which is also translocated to nuclear. During the SARS-CoV-2 infection, spike protein (S-protein) from SARS-CoV-2 suppress megalin expression which leads to the decrease of uptake of vitamin D. As the result, activated vitamin D and VDR translocation is diminished in both proximal and distal tubular cells.

the kidneys of infected mice according to immunochemical staining analysis, increased mRNA levels of these enzymes were observed. CYP27B1 has been reported to be negatively regulated by VDR translocation, which is consistent with our data showing elevated CYP27B1 mRNA levels in the SARS-CoV-2 group. Unexpectedly, on the other hand, CYP24A1 mRNA was elevated in infected mice even though CYP24A1 is reported to be regulated positively by VDR. The VDR translocation to nuclei was mainly observed in distal tubule. Therefore, the regulation of CYP24A1 expression in proximal tubule might be associated with other mechanism than VDR translocation. CYP24A1 has been reported to be upregulated with oxidative stress induced by high glucose[47] and FGF23/Klotho axis[48,49]. A previous study has reported that oxidative stress induces a decrease in the renal expression of *CYP27B1* and an increase in *CYP24A1* mRNA in kidneys damaged by lead, even when VDR showed decreased localization in the nucleus[50]. In diabetic rats[51], *CYP24A1* and *CYP27B1* mRNA levels are increased. Additionally, elevated mRNA expression levels of *CYP24A1*, *CYP27B1*, and *VDR* have been observed in patients with CKD and severe inflammation[52]. These results suggest that vitamin D metabolism in the kidney is regulated by a complicated mechanism to maintain homeostasis, whereby the protein levels of CYP24A1 and CYP27B1 may be normal, even when VDR localization is suppressed.

However, in the present study, the serum 25(OH)D and $1,25(OH)_2D$ levels in SARS-CoV-2-infected mice were similar to those in vehicle-treated mice. This suggests that serum vitamin D levels are maintained by vitamin D activation in tissues other than kidneys. Human mammary epithelial cells express megalin, cubilin, and CYP27B1 and can generate $1,25(OH)_2D$ from 25(OH)D[53]. Immune cells such as macrophages, dendritic cells, T lymphocytes, and B lymphocytes express vitamin D-activating enzymes and produce $1,25(OH)_2D$ within the innate and adaptive immune systems[54]. Furthermore, thyroid hormones are associated with $1,25(OH)_2D$ levels and the suppression of CYP27B1 expression[55]. Since serum vitamin D levels are regulated in a complex manner by extrarenal tissues, SARS-CoV-2 infection may not affect the systemic role of vitamin D. However, we cannot reject the possibility that AKI may affect the local role of vitamin D in the kidney and immune modulation. Vitamin D equilibrates the balance between T helper (Th) 1 and Th2 dells and reducing inflammation[56]. Treatment of T cell with active vitamin D inhibits the secretion of the proinflammatory Th1 cytokines (i.e., TNF-α) but promotes the production of anti-inflammatory Th2 cytokines (i.e., IL-4 and IL-10)[57]. This is consistent with the elevated TNF-α and the reduced IL-4 expression of our data. In contrast, elevated IL-10 levels were observed in SARS-CoV-2 infected mice even though this is an anti-inflammatory cytokine. It has been reported that endogenous IL-10 is upregulated in the kidney of unilateral ureteral obstruction mice and knockout of IL-10 leads to more severe inflammatory response and renal fibrosis[58]. IL-10 can be upregulated to play a role in renal protection through anti-inflammatory responses in the body. Vitamin D also suppresses

inflammatory TH17 activity and increases the expression of genes typical of regulatory T cells, which suppress proinflammatory responses[59]. These findings suggest that local vitamin D deficiency affects the inflammatory response in the kidneys and is associated with poor kidney outcomes. To evaluate vitamin D levels in kidney is needed for future task to argue this hypothesis. A study on COVID-19 survivors suggested that the estimated glomerular filtration rate of post-AKI COVID-19 survivors declines earlier than that of non-infected controls and that this tendency is observed strongly in the group of survivors hospitalized or admitted to intensive care[60]. In the present study, renal interstitial fibrosis was observed in mice 7 days after SARS-CoV-2 infection, which could be associated with chronic kidney disease. Further studies are needed to evaluate the effects of reduced megalin levels in the proximal tubules of patients with COVID-19 on renal outcomes and long-term renal sequelae.

In our study, we evaluated the sex difference of sensitivity to AKI associated with SARS-CoV-2 infection because some studies show a resistance to models of AKI in females than males[61]. Present study showed no tendency in the difference between male and female. It seems that SARS-CoV-2 infection induces AKI both in male and female. However, future research should validate the difference with sex with using a sufficient number of mice.

In conclusion, we confirmed decreased megalin levels at the renal brush border in SARS-CoV-2-infected hACE2-Tg mice. Furthermore, SARS-CoV-2 infection affected vitamin D-regulated gene expression in the kidney but did not affect blood vitamin D levels. Therefore, the local role of vitamin D in the kidneys should be evaluated to clarify the long-term effects of SARS-CoV-2 infection in animal models and patients with COVID-19.

Methods

Animal studies

The experimental procedures complied with the regulations for the management of experimental animals, and were approved by the Kitasato University Institutional Animal Care and Use Committee (approval numbers: 2020-8, 2021-9, and 2022-9) and the Genetic Modification Experiment Safety Committee (approval numbers 4557 and 5205), and all operations complied with the regulations for the management of experimental animals. The study was conducted in accordance with the ARRIVE guidelines. Heterozygous K18-hACE2 transgenic mice[62] were purchased from Jackson Laboratory (Bar Harbor, ME, USA). The SARS-CoV-2 strain hCoV-19/Japan/TY/WK-521 strain (WK-521, Pango Lineage A), isolated from patients with COVID-19[63], was provided by The National Institute of Infectious Diseases (Tokyo, Japan). Twelve-week-old male and female K18-hACE2 mice were inoculated intranasally with 5×10^4 plaque-forming unit of SARS-CoV-2 in a volume of 20 µL Dulbecco's modified eagle medium (DMEM; Fujifilm Wako Pure Chemical, Osaka, Japan) supplemented with 2% fetal bovine serum (Life Technologies, Carlsbad, CA, USA) and antibiotics (100 IU/mL penicillin and 100 µg/mL streptomycin; Fujifilm Wako Pure Chemical). Both male and female mice in the vehicle group received 20 µL of DMEM. Two to seven days after infection, kidneys were harvested from each mouse for further analysis. The experiments were performed at an animal biosafety Level 3 facility.

Renal histology assessment

Tissue preparation and sectioning were performed as previously described[64]. Sections were processed for hematoxylin and eosin (H&E) and Masson's trichrome staining according to standard protocols. The fibrosis area in Masson's trichrome staining from randomly selected regions (×100 magnification) were quantified using ImageJ software (v1.48, NIH) in each mouse. Periodic acid-Schiff staining was performed according to the manufacturer's instructions (Muto Pure Chemicals, Tokyo, Japan). The percentage of glomerular congestion was calculated from fifty randomly chosen glomeruli. The capillary congestion area from three high-power fields (×400) and the luminance of the brush border from hundred randomly chosen tubules were quantified using ImageJ software in each mouse.

Immunohistochemistry and immunofluorescence

For immunoperoxidase labeling, paraffin-embedded sections were incubated with primary antibodies against SARS-CoV-2 spike protein (40,589-T62, Sino Biological, Beijing, China, 1:200), megalin (ab76969, Abcam, Cambridge, MA, USA, 1:2000), NGAL (AF1857, R&D systems, Minneapolis, MN, USA, 1:50), KIM-1 (AF1817, R&D systems, 1:40), PCNA (2586, Cell Signaling Technology, Danvers, MA, USA, 1:2000), CYP24A1 (PB9547, BOSTER, Pleasanton, CA, USA, 1:50), CYP27B1 (sc-515903, Santa Cruz Biotechnology, Dallas, TX, USA, 1:50) and ACE2 (AF933, R&D systems, 1:25) at 4 °C overnight, followed by incubation with peroxidase-conjugated secondary antibody for 1 h. Peroxidase activity was then visualized with a 3,3′-diaminobenzidine substrate kit (Nichirei Biosciences, Inc., Tokyo, Japan), counterstained with Mayer's hematoxylin, and examined under a light microscope. Megalin- or PCNA-positive areas were quantified using ImageJ software from five randomly chosen cortical fields (×200), and the percentage of the stained area was measured. For immunofluorescence labeling, renal paraffin sections were incubated with primary antibodies against VDR (12,550, Cell Signaling Technology, 1:300) and phosphorylated H2AX (Ser139, γ-H2AX, Cell Signaling Technology, 1:400) at 4 °C overnight, followed by incubation with secondary antibodies, with or without LTL (Vector Laboratories, Newark, CA, USA, 1:200), a proximal tubule marker, for 1 h at room temperature. Images were captured using the Keyence all-in-one system (Keyence, Osaka, Japan). The number of VDR-positive nucleus were counted from three randomly chosen fields (×100 magnification) for each mouse. The percentage of γ-H2AX-positive cells was determined by counting positive cells and dividing them by the number of LTL-positive tubules in at least five photomicrographs (×100 magnification) by two blinded observers.

Gene	Primer sequence
Lrp2	Forward 5′-CGTTTGGACTCACCGTTTTT-3′
	Reverse 5′-TCAGCATCGTACGCTTTCAC-3′
ACTB	Forward 5′-CCCGCGAGCACAGCTTCTTTG-3
	Reverse 5′-ACATGCCGGAGCCGTTGTCGAC-3′
VDR	Forward 5′-GCATCCAAAAGGTCATCGGC-3′
	Reverse 5′-AGCGCAACATGATCACCTCA-3′
CYP27B1	Forward 5′-GCCGAGACTGGGATCAGATG-3′
	Reverse 5′-TGATGCCCAGACGGCATATC-3′
CYP24A1	Forward 5′-CCCCAAGTGCAACAGAGACT-3′
	Reverse 5′-CCGAGTTGTGAATGGCACAC-3′
TNFA	Forward 5′-CCCTCCTGGCCAACGGCATG-3′
	Reverse 5′-TCGGGGCAGCCTTGTCCCTT-3′
IL4	Forward 5′-ACAGGAGAAGGGACGCCAT-3′
	Reverse 5′-GAAGCCCTACAGACGAGCTCA-3′
IL10	Forward 5′-CACAAAGCAGCCTTGCAGAA -3′
	Reverse 5′-AGAGCAGGCAGCATAGCAGTG -3′

Table 2. Primer sequences for qPCR.

In situ hybridization (ISH)

To detect SARS-CoV-2 RNA in the lungs and kidneys, ISH was performed using the RNAscope 2.5 HD Reagent Kit-RED (Advanced Cell Diagnostics, Hayward, CA, USA) following the manufacturer's instructions. After peroxidase blocking with 0.5% hydrogen peroxide, the sections were heated in an antigen retrieval buffer and digested with the proteinase provided in the kit. Sections were incubated in an ISH target probe: V-nCov2019-S (RNAscpoe Probe cat.848561), Mm-Ppib (RNAscpoe Probe cat.313911), and a negative control probe (RNAscpoe Probe cat845701) at 40 °C in a hybridization oven for 2 h. After washing the sections, the ISH signal was amplified using the preamplifier provided in the kit, amplifier-conjugated to alkaline phosphatase, and incubated with 3,3′-diaminobenzidine for visualization at room temperature. The sections were counterstained with hematoxylin and examined under a light microscope.

Real-time reverse transcription-PCR (q-RT-PCR)

Total RNA was purified from the mouse kidney cortices using ISOGEN II (NIPPON GENE, Tokyo, Japan). The purity and concentration were determined by measuring the optical density at 260 and 280 nm, respectively. Using the purified RNA, reverse transcription reaction was performed using the Prime Script RT-PCR kits (Takara Bio, Shiga, Japan). The primers used for real-time PCR are listed in Table 2. PCR was performed on a 7500 Real-Time PCR System (Applied Biosystems) using Power SYBR Green (Applied Biosystems) as previously described[65]. The mRNA expression of the target genes was normalized to that of β-actin (ACTB) using the delta-delta Ct method and the vehicle group values were expressed as 1.

Determination of serum 25(OH)D or 1,25(OH)$_2$D levels using enzyme-linked immunosorbent assay

Enzyme-linked immunosorbent assay kits for serum 25(OH)D (ab213966, Abcam) and 1,25(OH)$_2$D (NBP2-82,432, Novus Biologicals, Littleton, CO, USA) were used to determine serum 25(OH)D and 1,25(OH)$_2$D levels, according to the manufacturer's instructions.

Statistical analysis

All data are reported as the mean ± SD. GraphPad Prism 8.4.3 (GraphPad Software, San Diego, CA, USA) was used for all the statistical analyses. Comparisons between infected and vehicle-treated mice were performed using the Mann–Whitney U test to assess differences. Other data were analyzed using analysis of variance (ANOVA) with post hoc comparisons using Tukey's test. Statistical significance was set at $P < 0.05$.

Data availability

All data supporting the findings of this study are available within the paper.

Received: 25 January 2024; Accepted: 4 October 2024
Published online: 16 October 2024

References

1. Mohamed, M. M. B. et al. Acute kidney injury associated with coronavirus disease 2019 in urban new orleans. *Kidney* **1**, 614–622 (2020).
2. Chan, L. et al. AKI in hospitalized patients with COVID-19. *J. Am. Soc. Nephrol.* **32**, 151–160 (2021).
3. Robbins-Juarez, S. Y. et al. Outcomes for patients with COVID-19 and acute kidney injury: A systematic review and meta-analysis. *Kidney Int Rep.* **5**, 1149–1160 (2020).

4. Naicker, S. et al. The Novel Coronavirus 2019 epidemic and kidneys. *Kidney Int.* **97**, 824–828 (2020).
5. Durvasula, R., Wellington, T., McNamara, E. & Watnick, S. COVID-19 and kidney failure in the acute care setting: Our experience from seattle. *Am. J. Kidney Dis.* **76**, 4–6 (2020).
6. Santoriello, D. et al. Postmortem kidney pathology findings in patients with COVID-19. *J. Am. Soc. Nephrol.* **31**, 2158–2167 (2020).
7. Akilesh, S. et al. Multicenter Clinicopathologic Correlation of Kidney Biopsies Performed in COVID-19 Patients Presenting With Acute Kidney Injury or Proteinuria. *Am. J. Kidney Dis.* **77**, 82–93 (2021).
8. Mohamed, M. M. B. & Velez, J. C. Q. Proteinuria in COVID-19. *Clin Kidney J.* **14**, i40–i47 (2021).
9. Su, H. et al. Renal histopathological analysis of 26 postmortem findings of patients with COVID-19 in China. *Kidney Int.* **98**, 219–227 (2020).
10. Fisher, M. et al. AKI in hospitalized patients with and without COVID-19: A comparison study. *J. Am. Soc. Nephrol.* **31**, 2145–2157 (2020).
11. Cheng, Y. et al. Kidney disease is associated with in-hospital death of patients with COVID-19. *Kidney Int.* **97**, 829–838 (2020).
12. Chaudhri, I. et al. Association of proteinuria and hematuria with acute kidney injury and mortality in hospitalized patients with COVID-19. *Kidney Blood Press. Res.* **45**, 1018–1032 (2020).
13. Kazemi, A. et al. Association of vitamin D status with SARS-CoV-2 infection or COVID-19 severity: A systematic review and meta-analysis. *Adv. Nutr.* **12**, 1636–1658 (2021).
14. Camargo, C. A. Jr. et al. Cord-blood 25-hydroxyvitamin D levels and risk of respiratory infection, wheezing, and asthma. *Pediatrics.* **127**, e180-187 (2011).
15. Bikle, D. D. Vitamin D regulation of immune function during covid-19. *Rev. Endocr. Metab. Disord.* **23**, 279–285 (2022).
16. Costagliola, G. et al. Nutraceuticals in viral infections: An overview of the immunomodulating properties. *Nutrients* **13**, 2410 (2021).
17. Murai, I. H. et al. Effect of a single high dose of vitamin D3 on hospital length of stay in patients with moderate to severe COVID-19: A randomized clinical trial. *JAMA* **325**, 1053–1060 (2021).
18. Schuster, I. Cytochromes P450 are essential players in the vitamin D signaling system. *Biochim. Biophys. Acta.* **1814**, 186–199 (2011).
19. Holick, M. F. Sunlight and vitamin D for bone health and prevention of autoimmune diseases, cancers, and cardiovascular disease. *Am. J. Clin. Nutr.* **80**, 1678S-1688S (2004).
20. Yin, K. & Agrawal, D. K. Vitamin D and inflammatory diseases. *J Inflamm. Res.* **7**, 69–87 (2014).
21. Holick, M. F. Vitamin D deficiency. *N. Engl. J. Med.* **357**, 266–281 (2007).
22. Jones, G., Prosser, D. E. & Kaufmann, M. 25-Hydroxyvitamin D-24-hydroxylase (CYP24A1): Its important role in the degradation of vitamin D. *Arch. Biochem. Biophys.* **523**, 9–18 (2012).
23. Graidis, S., Papavramidis, T. S. & Papaioannou, M. Vitamin D and acute kidney injury: A two-way causality relation and a predictive, prognostic, and therapeutic role of vitamin D. *Front Nutr.* **7**, 630951 (2020).
24. Bosworth, C. & de Boer, I. H. Impaired vitamin D metabolism in CKD. *Semin. Nephrol.* **33**, 158–168 (2013).
25. Nykjaer, A. et al. Cubilin dysfunction causes abnormal metabolism of the steroid hormone 25(OH) vitamin D(3). *Proc. Natl. Acad. Sci. USA* **98**, 13895–13900 (2001).
26. Saito, A., Pietromonaco, S., Loo, A. K. & Farquhar, M. G. Complete cloning and sequencing of rat gp330/"megalin," a distinctive member of the low density lipoprotein receptor gene family. *Proc. Natl. Acad. Sci. USA* **91**, 9725–9729 (1994).
27. Hjalm, G. et al. Cloning and sequencing of human gp330, a Ca(2+)-binding receptor with potential intracellular signaling properties. *Eur. J. Biochem.* **239**, 132–137 (1996).
28. Nykjaer, A. et al. An endocytic pathway essential for renal uptake and activation of the steroid 25-(OH) vitamin D3. *Cell* **96**, 507–515 (1999).
29. Werion, A. et al. SARS-CoV-2 causes a specific dysfunction of the kidney proximal tubule. *Kidney Int.* **98**, 1296–1307 (2020).
30. Omer, D. et al. Human kidney spheroids and monolayers provide insights into SARS-CoV-2 renal interactions. *J. Am. Soc. Nephrol.* **32**, 2242–2254 (2021).
31. Wang, W. G., Sun, W. X., Gao, B. S., Lian, X. & Zhou, H. L. Cell cycle arrest as a therapeutic target of acute kidney injury. *Curr. Protein Pept. Sci.* **18**, 1224–1231 (2017).
32. Kellum, J. A. & Chawla, L. S. Cell-cycle arrest and acute kidney injury: the light and the dark sides. *Nephrol. Dial. Transplant.* **31**, 16–22 (2016).
33. Kilari, S., Yang, B., Sharma, A., McCall, D. L. & Misra, S. Increased transforming growth factor beta (TGF-beta) and pSMAD3 signaling in a murine model for contrast induced kidney injury. *Sci. Rep.* **8**, 6630 (2018).
34. Hirsch, J. S. et al. Acute kidney injury in patients hospitalized with COVID-19. *Kidney Int.* **98**, 209–218 (2020).
35. Chavez-Valencia, V., Orizaga-de-la-Cruz, C. & Lagunas-Rangel, F. A. Acute kidney injury in COVID-19 patients: Pathogenesis, clinical characteristics, therapy, and mortality. *Diseases* **10**, 53 (2022).
36. Farkash, E. A., Wilson, A. M. & Jentzen, J. M. Ultrastructural evidence for direct renal infection with SARS-CoV-2. *J. Am. Soc. Nephrol.* **31**, 1683–1687 (2020).
37. Zhou, P. et al. A pneumonia outbreak associated with a new coronavirus of probable bat origin. *Nature* **579**, 270–273 (2020).
38. Mizuiri, S. & Ohashi, Y. ACE and ACE2 in kidney disease. *World J. Nephrol.* **4**, 74–82 (2015).
39. George, S. et al. Evidence for SARS-CoV-2 Spike Protein in the Urine of COVID-19 Patients. *Kidney* **2**, 924–936 (2021).
40. Silva-Aguiar, R. P. et al. SARS-CoV-2 spike protein inhibits megalin-mediated albumin endocytosis in proximal tubule epithelial cells. *Biochim. Biophys. Acta Mol. Basis Dis.* **1868**, 166496 (2022).
41. Biemesderfer, D. Regulated intramembrane proteolysis of megalin: linking urinary protein and gene regulation in proximal tubule?. *Kidney Int.* **69**, 1717–1721 (2006).
42. Li, Y., Cong, R. & Biemesderfer, D. The COOH terminus of megalin regulates gene expression in opossum kidney proximal tubule cells. *Am. J. Physiol. Cell Physiol.* **295**, C529-537 (2008).
43. Fatah, H. et al. Reduced proximal tubular expression of protein endocytic receptors in proteinuria is associated with urinary receptor shedding. *Nephrol. Dial. Transplant.* **33**, 934–943 (2018).
44. Maritzen, T., Rickheit, G., Schmitt, A. & Jentsch, T. J. Kidney-specific upregulation of vitamin D3 target genes in ClC-5 KO mice. *Kidney Int.* **70**, 79–87 (2006).
45. Xu, Y. et al. The importance of vitamin d metabolism as a potential prophylactic, immunoregulatory and neuroprotective treatment for COVID-19. *J. Transl. Med.* **18**, 322 (2020).
46. de Braganca, A. C. et al. Vitamin D deficiency aggravates ischemic acute kidney injury in rats. *Physiol. Rep.* **3**, e12331 (2015).
47. Tourigny, A. et al. CYP24A1 exacerbated activity during diabetes contributes to kidney tubular apoptosis via caspase-3 increased expression and activation. *PLoS One.* **7**, e48652 (2012).
48. Wolf, M. Forging forward with 10 burning questions on FGF23 in kidney disease. *J. Am. Soc. Nephrol.* **21**, 1427–1435 (2010).
49. Leaf, D. E., Wolf, M. & Stern, L. Elevated FGF-23 in a patient with rhabdomyolysis-induced acute kidney injury. *Nephrol. Dial. Transplant.* **25**, 1335–1337 (2010).
50. BaSalamah, M. A. et al. Vitamin D alleviates lead induced renal and testicular injuries by immunomodulatory and antioxidant mechanisms in rats. *Sci. Rep.* **8**, 4853 (2018).
51. Mazanova, A. et al. The link between vitamin D status and NF-kappaB-associated renal dysfunction in experimental diabetes mellitus. *Biochim. Biophys. Acta Gen. Subj.* **1866**, 130136 (2022).

52. Zehnder, D. et al. Reduction of the vitamin D hormonal system in kidney disease is associated with increased renal inflammation. *Kidney Int.* **74**, 1343–1353 (2008).
53. Rowling, M. J., Kemmis, C. M., Taffany, D. A. & Welsh, J. Megalin-mediated endocytosis of vitamin D binding protein correlates with 25-hydroxycholecalciferol actions in human mammary cells. *J. Nutr.* **136**, 2754–2759 (2006).
54. Baeke, F., Takiishi, T., Korf, H., Gysemans, C. & Mathieu, C. Vitamin D: modulator of the immune system. *Curr. Opin. Pharmacol.* **10**, 482–496 (2010).
55. Kozai, M. et al. Thyroid hormones decrease plasma 1alpha,25-dihydroxyvitamin D levels through transcriptional repression of the renal 25-hydroxyvitamin D3 1alpha-hydroxylase gene (CYP27B1). *Endocrinology* **154**, 609–622 (2013).
56. Daniel, C., Sartory, N. A., Zahn, N., Radeke, H. H. & Stein, J. M. Immune modulatory treatment of trinitrobenzene sulfonic acid colitis with calcitriol is associated with a change of a T helper (Th) 1/Th17 to a Th2 and regulatory T cell profile. *J. Pharmacol. Exp. Ther.* **324**, 23–33 (2008).
57. Sapartini, G., Wong, G. W. K., Indrati, A. R., Kartasasmita, C. B. & Setiabudiawan, B. The association between vitamin D, interleukin-4, and interleukin-10 levels and CD23+ expression with bronchial asthma in stunted children. *Biomedicines* **11**, 2542 (2023).
58. Jin, Y. et al. Interleukin-10 deficiency aggravates kidney inflammation and fibrosis in the unilateral ureteral obstruction mouse model. *Lab. Invest.* **93**, 801–811 (2013).
59. Azrielant, S. & Shoenfeld, Y. Vitamin D and the immune system. *Isr. Med. Assoc. J.* **19**, 510–511 (2017).
60. Bowe, B., Xie, Y., Xu, E. & Al-Aly, Z. Kidney outcomes in long COVID. *J. Am. Soc. Nephrol.* **32**, 2851–2862 (2021).
61. Curtis, L. M. Sex and gender differences in AKI. *Kidney* **5**, 160–167 (2024).
62. McCray, P. B. Jr. et al. Lethal infection of K18-hACE2 mice infected with severe acute respiratory syndrome coronavirus. *J. Virol.* **81**, 813–821 (2007).
63. Matsuyama, S. et al. Enhanced isolation of SARS-CoV-2 by TMPRSS2-expressing cells. *Proc. Natl. Acad. Sci. U. S. A.* **117**, 7001–7003 (2020).
64. Kurosaki, Y. et al. Oxidative stress increases megalin expression in the renal proximal tubules during the normoalbuminuric stage of diabetes mellitus. *Am. J. Physiol. Renal Physiol.* **314**, F462–F470 (2018).
65. Kurosaki, Y. et al. In vitro study on effect of bardoxolone methyl on cisplatin-induced cellular senescence in human proximal tubular cells. *Mol. Cell. Biochem.* **477**, 689–699 (2022).

Acknowledgements

We would like to thank Editage (www.editage.jp) for English language editing.

Author contributions

Y.K., H.K., H.H., and M.K. provided conception and design of research; Y.K., T.M., T.U., and M.I. performed experiments; Y.K., T.M., F.K., R.K., and S.T. analyzed data; Y.K., T.U., F.K., R.K., T.I., N.I., H.K., H.H., and M.K. interpreted results of experiments; Y.K. and T.M. prepared figures; Y.K. drafted manuscript; Y.K., T.U., T.I., N.I., H.K., H.H., and M.K. edited and revised manuscript; Y.K., T.M., T.U., F.K., R.K., S.T., M.I., T.I., N.I., H.K., H.H., and M.K. approved final version of manuscript.

Funding

School of Allied Health Sciences,Kitasato University,Grant-in-Aid for Research Project No. 2022-1020,COV-ID-19 Kitasato Project

Competing interests

The authors declare no competing interests.

Additional information

Supplementary Information The online version contains supplementary material available at https://doi.org/10.1038/s41598-024-75338-9.

Correspondence and requests for materials should be addressed to M.K.